JCTC Journal of Chemical Theory and Computation

pubs.acs.org/JCTC Article

Reliable Gas Phase Reaction Rates at Affordable Cost by Means of the Parameter-Free JunChS-F12 Model Chemistry

Vincenzo Barone,* Jacopo Lupi, Zoi Salta, and Nicola Tasinato

Cite This: *J. Chem. Theory Comput.* 2023, 19, 3526−3537 Read Online

ACCESS | Metrics & More | Article Recommendations | Supporting Information

ABSTRACT: A recently developed strategy for the computation at affordable cost of reliable barrier heights ruling reactions in the gas phase (junChS, [Barone, V.; et al. *J. Chem. Theory Comput.* **2021**, *17*, 4913−4928]) has been extended to the employment of explicitly correlated (F12) methods. A thorough benchmark based on a wide range of prototypical reactions shows that the new model (referred to as junChS-F12), which employs cost-effective revDSD-PBEP86-D3(BJ) reference geometries, has an improved performance with respect to its conventional counterpart and outperforms the most well-known model chemistries without the need of any empirical parameter and at an affordable computational cost. Several benchmarks show that revDSD-PBEP86-D3(BJ) structures and force fields provide zero point energies and thermal contributions, which can be confidently used, together with junChS-F12 electronic energies, for obtaining accurate reaction rates in the framework of the master equation approach based on the ab initio transition-state theory.

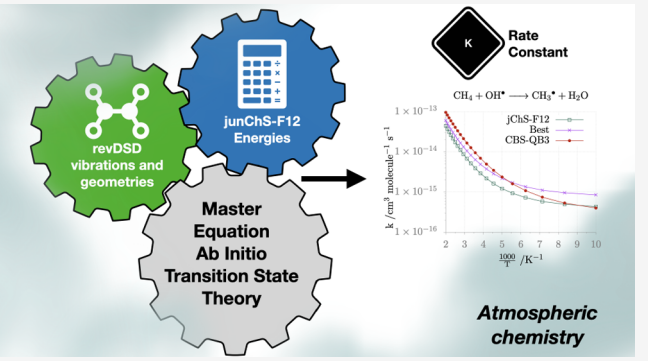

INTRODUCTION

The main focus of atmospheric chemistry is the descritption and analysis of Earth's atmosphere in terms of the underlying physical-chemical processes controlling the sources and fate of the different chemical species produced by natural or anthropogenic emissions. However, despite significant progress, the interpretation of atmospheric processes in terms of the underlying chemistry faces against a number of difficulties mainly related to the interplay between chemical composition and meteorological/transport processes.

In the last years, the increasing synergism among the major pillars of atmospheric chemistry, namely observational measurements, laboratory investigation, and atmospheric modeling,[1,2] is providing invaluable insights into the intricate phenomena occurring in the atmosphere. In this framework, computational chemistry can be of considerable help for gaining additional information about ground and excited state properties of chemical species, their photochemical pathways, chemical reaction mechanisms, and rate coefficients.[3] In particular, kinetic and mechanistic features of reactions are usually interpreted employing the Arrhenius equation to describe the variation of the rate constant with temperature[4]

$$k(T) = A\exp\left(-\frac{E_a}{RT}\right) \quad (1)$$

where A is the pre-exponential or frequency factor (which may involve a small dependence on temperature) and E_a is the activation energy. While more precise definitions are available,[5,6] the activation energy is usually interpreted as the minimum energy (kinetic plus potential, relative to the lowest state of reactants) that reactants must have to form products and the pre-exponential factor is a measure of the rate at which collisions occur. If a reaction obeys the Arrhenius equation, then a plot of ln k versus $\frac{1}{T}$ should produce a straight line, whose slope and intercept at the origin are $-\frac{E_a}{R}$ and A, respectively. However, many reactions of wide current interest do not obey the Arrhenius equation and/or have negative activation energies (rate constants that decrease when the temperature is increased).[7,8] At the same time, the experimental characterization of several reactions of atmospheric interest is made difficult by the involvement of highly reactive species, such as free radicals or ions.

Under such circumstances, accurate yet feasible quantum chemical approaches are needed. The main factors determining the accuracy of computed rate constants are the reaction energies and the energy barriers for all the elementary steps involved in the reaction under investigation. In the absence of species with a strong multireference character and/or non-

Received: March 27, 2023
Published: May 31, 2023

adiabatic effects, the coupled cluster (CC) approach delivers accurate results provided that the most important classes of excitations are included together with complete basis set (CBS) extrapolation, core−valence (CV) correlation, and, if needed, other minor effects (scalar relativistic, diagonal non-Born−Oppenheimer, spin−orbit). Due to an effective error compensation, single, double, and (perturbative estimates of) triple excitations are usually sufficient, leading to the CCSD(T)-CBS+CV model, which is often considered the gold standard of contemporary computational chemistry. At this level, chemical accuracy (4 kJ mol^{-1}) can be reached either by employing large basis sets,[9] resorting to empirical parameters in conjunction with smaller basis sets (e.g., G4,[10] CBS-QB3[11]), or employing explicitly correlated (F12) models (e.g., W1-F12[12] or SVECV-f12[13]). The most reliable protocols (e.g., HEAT,[14] W4,[12] and their explicitly correlated HEAT-F12 and W4-F12[15] variants) further increase the overall accuracy (below 1 kJ mol^{-1}) including additional (expensive) contributions. In this connection it should be pointed out that the latter protocols push also geometry optimizations to the limit, whereas, at the other extreme, G4 and CBS-QB3 schemes employ B3LYP geometries, whose accuracies are often unsatisfactory.[10,16]

Next, zero point energies (ZPEs) and finite temperature contributions (FTCs) come into play, which are determined by geometries and vibrational frequencies. In this connection, effective approaches going beyond the standard rigid rotor/harmonic oscillator (RRHO) model are needed especially when light atoms or hindered rotors are involved. Finally, barrierless entrance or exit channels are often encountered for reactions in the gas phase, which require the accurate description of noncovalent interactions.

Based on these premises, we have developed a composite method, referred to as the "cheap" scheme (ChS) and devoid of any empirical parameter, which has provided accurate structural and energetic data at nonprohibitive costs.[17−19] In conjunction with geometries and harmonic frequencies computed by double-hybrid functionals, ChS has given promising results also for the activation energies of some reactions of astrochemical interest.[20−24] In analogy with the W1X[25] and SVECV-f12[13] composite methods, ChS employs the second order Møller−Plesset perturbation theory (MP2)[26] for estimating the CV correlation. A further reduction of the computational cost is achieved by performing, in accord with the correlation consistent composite approach (ccCA),[27,28] also the CBS extrapolation at the MP2 level. Quite recently, an improved variant (referred to as the jun-Cheap scheme, junChS) has been introduced, which, thanks to the use of the "june" partially augmented basis sets of the "calendar" family,[29] provides accurate results also for noncovalent interactions[30,31] and activation energies.[16]

In the present paper we perform a comprehensive benchmark of the latest member of the "cheap" family of composite methods, junChS-F12,[32,33] for several classes of reactions for which accurate reference results are available or have been purposely computed. We will show that, thanks to the replacement of conventional post-Hartree−Fock methods by their explicitly correlated (F12) counterparts, this model chemistry improves the accuracy of previous variants, strongly reducing the uncertainty of CBS extrapolation without any excessive increase of computational requirements. Together with electronic energies, we analyze also the roles of geometries, ZPEs, and FTCs in tuning reaction rates in the framework of the master equation approach based on the ab initio transition-state theory (ME/AITST).[34−36]

COMPUTATIONAL DETAILS

All the composite schemes discussed in the present work employ the cc-pV(n+d)Z (hereafter nZ)[37] or jun-cc-pV(n+d)Z (hereafter jnZ)[29] families of basis sets.

The geometrical parameters and harmonic vibrational frequencies of energy minima and first-order saddle points (transition states) are obtained employing analytical gradients and Hessians computed by the revDSD-PBEP86-D3(BJ) double-hybrid functional[38,39] in conjunction with the j3Z basis set (this combination of functional and basis set will be referred to in the following as rDSD).

At those geometries, single point energy evaluations are performed by the explicitly correlated coupled cluster method, including single, double, and (perturbatively) triple excitations (CCSD(T)-F12)[40,41] within the frozen-core approximation and in conjunction with the j3Z basis set. Next, CBS extrapolation, CV correlation, and, possibly, other minor terms are added at different levels depending on the specific model chemistry. Finally, the experimental values of spin−orbit couplings are employed for O, OH, SH, and Cl radicals, lowering their electronic energies by 0.9, 0.8, 2.3, and 3.5 kJ mol^{-1}, respectively.[42]

All the DFT computations have been performed with the Gaussian code,[43] F12 calculations with the Molpro package[44] and CCSDT or CCSDT(Q) energy evaluations with the MRCC program.[45] Finally, diagonal Born−Oppenheimer Corrections (DBOC) and relativistic contributions have been computed by the CFOUR code.[46]

The junChS-F12 Model Chemistry. The junChS-F12 total electronic energies are obtained by the following recipe:

$$E_{\text{junChS-F12}} = E(\text{CCSD(T)-F12/j3Z}) + \Delta E^{\text{CBS}}_{\text{MP2-F12}} + \Delta E^{\text{CV}}_{\text{MP2-F12}} \quad (2)$$

where

$$\Delta E^{\text{CBS}}_{\text{MP2-F12}} = \frac{4^3 E(\text{MP2-F12/j4Z}) - 3^3 E(\text{MP2-F12/j3Z})}{4^3 - 3^3} - E(\text{MP2-F12/j3Z}) \quad (3)$$

and

$$\Delta E^{\text{CV}}_{\text{MP2-F12}} = E(\text{MP2-F12}^{\text{ae}}/\text{C3Z}) - E(\text{MP2-F12}^{\text{fc}}/\text{C3Z}) \quad (4)$$

In the above equations $\Delta E^{\text{CBS}}_{\text{MP2-F12}}$ is the MP2-F12 correlation energy extrapolated to the CBS limit using the n^{-3} formula[47] and $\Delta E^{\text{CV}}_{\text{MP2-F12}}$ is the MP2-F12 energy difference between all electron (ae) and frozen core (fc) calculations employing the cc-pwCVTZ basis set (C3Z).[48] At this level, the extrapolation of Hartree−Fock (HF) and correlation contributions is performed with the same equation and basis sets since several tests have shown that this simplified recipe has a negligible impact on the overall accuracy of the results.[27,28,30,32]

Derivation of eq 2 w.r.t. Cartesian coordinates leads to the junChS-F12 version of the so-called "gradient scheme" introduced by Gauss and co-workers[49,50] for geometry optimizations by composite methods

https://doi.org/10.1021/acs.jctc.3c00343
J. Chem. Theory Comput. 2023, 19, 3526−3537

$$\frac{dE_{\text{junChS-F12}}}{dx} = \frac{dE(\text{CCSD(T)-F12/j3Z})}{dx} + \frac{dE(\text{MP2-F12}^{\text{ae}}/\text{C3Z})}{dx} - \frac{dE(\text{MP2-F12}^{\text{fc}}/\text{C3Z})}{dx} \quad (5)$$

where, on the grounds of previous experience,[32,51] the CBS contribution can be safely neglected. To further extend the applicability of composite approaches to larger molecules, an effective solution is provided by the so-called "geometry" scheme.[52,53] This is based on the assumption that the additivity approximation can be directly applied to geometrical parameters and only requires geometry optimizations at several levels of theory. The different contributions are thus evaluated separately and then combined together. This approach will be used in the following sections to analyze the role of different geometries on the final evaluation of electronic energies (ΔGEOM contribution).

Additional Terms. Starting from junChS-F12 electronic energies, additional terms can be added to improve the accuracy of the final results (E_{Best}):

$$E_{\text{Best}} = E_{\text{junChS-F12}} + \Delta E_{\text{CBS}} + \Delta E_{\text{CV}} + \Delta E_{\text{fT}} + \Delta E_{\text{pQ}} + \Delta E_{\text{rel}} + \Delta E_{\text{DBOC}} \quad (6)$$

The CBS and CV contributions refer to the differences between evaluations of these terms at the CCSD(T)-F12 and MP2-F12 levels. The diagonal Born−Oppenheimer correction ΔE_{DBOC}[54−57] and the scalar relativistic contribution to the energy ΔE_{rel}[58,59] are computed at the HF-SCF/aug-cc-pVDZ and CCSD(T)/aug-cc-pCVDZ levels, after having checked their convergence with respect to contributions calculated with triple-ζ basis sets for a few stationary points. Finally, the corrections due to full treatment of triple (ΔE_{fT}) and perturbative treatment of quadruple (ΔE_{pQ}) excitations are computed, within the fc approximation, as energy differences between CCSDT and CCSD(T) and between CCSDT(Q) and CCSDT calculations employing the cc-pVTZ and cc-pVDZ basis set, respectively.

In the following, the method obtained including only the first three terms of eq 6 will be referred to as CBS+CV, whereas the method including all the terms of eq 6 will be referred to as *Best*. While straightforward generalizations of eq 4 would allow geometry optimizations at the CBS+CV and *Best* levels, this route has not been pursued here due to the negligible improvement over junChS-F12 in the former case and the lack of analytical gradient implementations for fT and pQ contributions in the latter case.

Zero Point Energy and Finite Temperature Contributions. Accurate determination of thermochemical and kinetic parameters by quantum chemical methods requires, in addition to electronic energies, also zero point energies (ZPE) and finite temperature contributions (FTC), which are usually obtained within the RRHO approximation, possibly employing empirical scaling factors.[60] In the present context, the use of empirical factors is avoided by resorting to generalized second order vibrational perturbation theory in conjunction with a separate treatment of large amplitude motions.[61,62] In fact, a resonance-free expression for ZPEs of energy minima and transition states,[63,64] an unsupervised smoothing procedure (HDCPT2) for fundamental frequencies[65] and a fully unsupervised detection and treatment of torsional motions (hindered rotor, HR, approximation)[66] have been implemented in the Gaussian code[43] and validated.[67] As a consequence a fully black-box procedure is available for taking into account all these contributions.

Next, partition functions can be computed by the so-called simple perturbation theory (SPT),[68] which retains the formal expression of the harmonic partition function, but employing the anharmonic ZPE and fundamental levels (Δ_i) issuing from HDCPT2 and HR computations.

$$Q_{\text{vib}} = \frac{\exp\left(-\frac{\text{ZPE}}{k_B T}\right)}{\prod_i \left[1 - \exp\left(-\frac{\Delta_i}{k_B T}\right)\right]} \quad (7)$$

This approximation provides results in remarkable agreement with accurate reference values and leads to analytical expressions for the different thermodynamic functions.[68]

Kinetic Models. Global and channel-specific rate constants can be computed solving the multiwell one-dimensional master equation using the chemically significant eigenvalues (CSEs) method within the Rice−Ramsperger−Kassel−Marcus (RRKM) approximation, as implemented in the MESS code.[41] The collisional energy transfer probability is described using the exponential down model[69] with a temperature dependent ΔE_{down} of $260 \times (T/298)^{0.875}$ cm^{-1} in an argon bath gas.[69]

For channels ruled by a distinct saddle point, rate coefficients are determined by conventional transition state theory (TST)[70] including tunneling as well as non classical reflection effects by the Eckart model.[71] Instead, rate constants for barrierless elementary reactions are computed by the phase space theory (PST).[72,73] The isotropic attractive potential V_{eff} entering the PST is described by a $\frac{C}{R^6}$ power law, whose C coefficient is obtained by fitting rDSD energies computed at various long-range distances between the fragments.

While the adopted models for the inclusion of tunneling and the description of barrierless entrance channels usually deliver qualitatively correct results, they neglect a number of effects (e.g., variational location of the TS, nonvanishing curvature of the reaction path, etc.), whose proper treatment would require more advanced models.[21,74] However, these models require, in turn, additional information besides the characterization of the stationary points governing each elementary step. As a consequence, we prefer to postpone these aspects after the reliability of the proposed approach for the structural and energetic properties of stationary points has been definitely assessed.

The rate constants of the overall reactions evaluated at different temperatures are fitted by the three-parameter modified Arrhenius equation proposed by Kooij:[75,76]

$$k(T) = A\left(\frac{T}{300}\right)^n \exp\left(-\frac{E_a}{RT}\right) \quad (8)$$

where A, n, and E_a are the fitting parameters, and R is the universal gas constant.

RESULTS AND DISCUSSION

The most widely employed reference results for reaction barriers are collected in the DBH24 compilation[77,78] containing results mostly obtained at the CCSDTQ5/CBS

https://doi.org/10.1021/acs.jctc.3c00343
J. Chem. Theory Comput. 2023, 19, 3526−3537

Table 1. Theoretical Values of the Barrier Heights (Not Including Spin−Orbit Correction and ZPE) in the DBH24 Compilation Obtained at Different Levels of Theory[a]

		forward/reverse barrier height				
	reactions	CC-F12a/j3Z	junChS-F12	fT+pQ	ref 78	Δanh
		heavy-atom transfer				
a1	$H^{\bullet} + N_2O \rightarrow OH^{\bullet} + N_2$	74.0/347.8 [74.2/347.4]	73.9/348.3	−1.4/−3.2	71.7/345.0	−0.2/−0.2
a2	$H^{\bullet} + ClH \rightarrow HCl + H^{\bullet}$	75.2/75.2 [75.9/75.9]	73.6/73.6	−0.55/−0.5	75.3/75.3	1.3/1.3
a3	$CH_3^{\bullet} + FCl \rightarrow CH_3F + Cl^{\bullet}$	29.9/250.4 [30.0/250.5]	29.9/251.3	−1.0/−1.2	28.2/251.0	−0.8/0.1
		nucleophilic substitution				
a4	$Cl^{-}\cdots CH_3Cl \rightarrow ClCH_3\cdots Cl^{-}$	56.2/56.2 [56.7/56.7]	56.2/56.2	−1.0/−1.0	56.1/56.1	0.1/0.1
a5	$F^{-}\cdots CH_3Cl \rightarrow FCH_3\cdots Cl^{-}$	14.3/122.5 [14.5/123.7]	14.6/123.7	−0.8/−0.9	14.4/123.1	0.0/0.0
a6	$OH^{-} + CH_3F \rightarrow HOCH_3 + F^{-}$	−11.8/73.5 [−11.1/74.0]	−8.9/74.8	−1.3/−1.4	−10.2/73.9	−0.4/0.0
		unimolecular and association				
a7	$H^{\bullet} + N_2 \rightarrow HN_2^{\bullet}$	61.4/45.8 [61.8/45.4]	60.8/46.3	0.5/0.7	60.1/44.4	−0.4/0.1
a8	$H^{\bullet} + C_2H_4 \rightarrow C_2H_5^{\bullet}$	9.1/177.1 [9.3/177.0]	8.3/176.6	−0.5/−0.6	7.2/174.7	−0.3/−0.2
a9	HCN ↔ HNC	199.6/137.8 [199.3/137.5]	201.2/138.6	−0.2/−0.6	201.1/137.3	0.1/0.1
		hydrogen transfer				
a10	$OH^{\bullet} + CH_4 \rightarrow CH_3^{\bullet} + H_2O$	27.1/82.2 [27.1/81.9]	27.7/83.3	−0.7/−0.6	28.1/82.0	1.0/0.9
a11	$H^{\bullet} + OH^{\bullet} \rightarrow H_2 + {}^3O$	46.3/56.9 [45.8/56.6]	46.6/57.6	−0.6/−1.0	44.8/54.9	0.7/0.8
a12	$H^{\bullet} + H_2S \rightarrow H_2 + HS^{\bullet}$	17.1/73.9 [17.6/73.6]	16.0/76.3	−0.5/−0.4	15.2/72.5	−0.5/−0.6

[a]F12b values are reported in square brackets. The contributions of full-triple and perturbative-quadruple excitations (fT+pQ) and the differences between anharmonic and harmonic ΔZPEs computed at the rDSD level (Δanh) are also given. All the values are in kJ mol^{-1}.

level by means of the W4 composite method[79] for a statistically representative set including 3 prototypes for each of the following classes of reactions: heavy atom transfer, nucleophilic substitution, unimolecular and association reactions, and hydrogen-transfer reactions.

Table 1 compares the reaction barriers computed at the junChS-F12 level to the reference values of ref 78. From a technical point of view, the results show that F12a and F12b variants of the CCSD-F12 method[41] provide comparable results, so that only F12a values will be discussed in detail in the following. As shown in Table 1, the CCSD(T)-F12/j3Z error is already on par with the best available composite methods[13] and is further slightly reduced adding CBS and CV contributions by inexpensive MP2-F12 computations. These trends confirm that two-point extrapolation at the MP2-F12 level is an effective route for estimating the CBS limit without introducing additional computational bottlenecks with respect to the underlying CCSD(T)-F12/j3Z reference. As a matter of fact, already for reactions involving two heavy atoms, junChS-F12 computations require no more than twice the time of the CCSD(T)-F12/jun-cc-pVTZ step and are 1 order of magnitude faster than their CBS+CV counterparts. It is also remarkable that all the energy barriers showing non-negligible errors have quite large contributions from full triple and perturbative quadruple excitations (fT+pQ), which are not included in the junChS-F12 approach nor in its CBS+CV counterpart. Table 1 collects also the differences between anharmonic and harmonic ZPE contributions to energy barriers (Δanh). While these terms (together with spin−orbit contributions) will be discussed in more detail in the following, we already point out that their contribution is sometimes comparable with that of (fT+pQ).

Two larger compilations of energy barriers are available for prototypical reactions involving the transfer of hydrogen (HTBH38/08[80]) and non-hydrogen atoms (NHTBH38/08[81]), respectively. However, the values not already included in the DBH24 set have been obtained at a lower computational level (W1[82]). In order to investigate the role of different effects on energy barriers we have computed *Best* values for all the reactions belonging to those two sets. It is noteworthy that rDSD energy barriers, although not directly used in the junChS model chemistries, show mean unsigned errors (MUEs) smaller than 8.0 kJ mol^{-1}, thus suggesting that the corresponding geometries should be sufficiently accurate for single-point energy evaluations at higher computational levels.

Figure 1 shows the errors issued from different model chemistries, whereas the corresponding energy barriers are given in Table S1 of the Supporting Information (SI). It is quite apparent that CBS extrapolation plays a much more important role in conventional composite methods (junChS) than in their explicitly correlated counterparts (junChS-F12). However, also in the latter case its inclusion (together with that of the CV contribution) is surely warranted in view of the quite negligible cost. As expected, the junChS-F12 model

https://doi.org/10.1021/acs.jctc.3c00343
J. Chem. Theory Comput. 2023, 19, 3526−3537

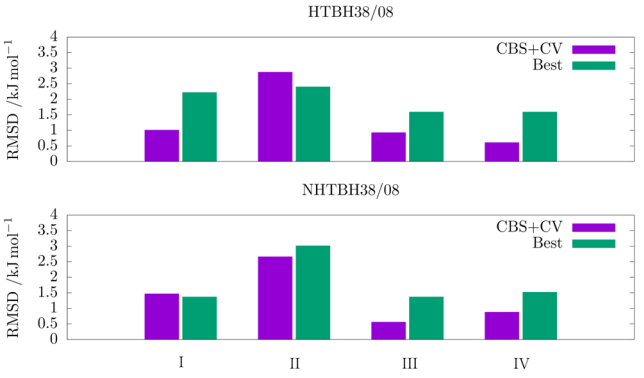

Figure 1. Root-mean-square deviations of different model chemistries from reference values (CBS+CV or *Best*) of energy barriers belonging to the HTBH38/08 and NHTBH38/08 compilations: junChS (I), junChS without MP2 CBS extrapolation (II), junChS-F12 (III) and junChS-F12 without MP2-F12 CBS extrapolation (IV).

shows smaller errors with respect to the reference values than the junChS approach, with both models clearly satisfying the requirements of chemical accuracy (i.e., errors within 4 kJ mol^{-1}) without the need of any empirical parameter.

Tables 2 and 3 show the contributions given by improved geometries (junChS-F12 vs rDSD referred to as ΔGEOM), core−valence correlation (CV−F12), triple excitations (fT), quadruple excitations (included perturbatively, pQ), diagonal Born−Oppenheimer corrections (DBOC), scalar relativistic contributions (rel), and spin−orbit couplings (ΔSO). The quality of rDSD geometries is confirmed by the small values of the ΔGEOM contributions, with the possible exception of reactions involving two doublet species (especially HT15 and HT16), where spin contamination effects can become non-negligible also for double-hybrid functionals.[83] Noted is that geometries optimized by hybrid functionals or MP2 (either UMP2 or ROMP2) methods produce significantly larger ΔGEOM contributions.[16,84]

In more general terms, the results collected in Tables 2 and 3 show that none of the contributions mentioned above can be neglected for reaching fully converged values. As already mentioned, this is also the case for anharmonic corrections to ZPEs (see Δanh in Table 1). In this connection, we recall that accurate ZPEs and thermal contributions can be obtained in the framework of the SPT[68] from HDCPT2[65] computations employing rDSD anharmonic force fields.[16,51] All in all, evaluation of electronic energies at the junChS-F12 level in conjunction with rDSD geometries and vibrational frequencies represents a reliable tool for the study of medium- to large-size systems in the absence of strong multireference effects.

RATE CONSTANTS

In this section, we analyze the performance of three composite schemes (junChS-F12, *Best* and the largely employed CBS-QB3 model[11]) for the computation of rate constants within the ME/AITST approach. To the purpose we have chosen at least one example for each of the main classes of reactions considered in the reference databases discussed in the preceding section. The selected reactions are $CH_4 + OH \rightarrow CH_3 + H_2O$ (HT4) and $H + PH_3 \rightarrow PH_2 + H_2$ (HT11) for hydrogen transfer; $Cl^- + CH_3Cl \rightarrow ClCH_3 + Cl^-$ (NHT10) for nucleophilic substitution; $HCN \rightarrow HNC$ (NHT19) for unimolecular isomerization, and $H + FH \rightarrow HF + H$ (NHT2) for heavy-atom transfer. While the original recipes have been used for the evaluation of ZPE and thermal effects in the CBS-QB3 method, rDSD geometries and VPT2 anharmonic frequencies have been used in junChS-F12 and *Best* computations in order to avoid any empirical scaling factor.

The reaction of OH with CH_4 (HT4) is very important in the Earth's troposphere since it accounts for about 90% of the total CH_4 sink.[85] The junChS-F12 and *Best* energy barriers are quite close (27.7 and 28.1 kJ mol^{-1}, respectively), whereas a

Table 2. Geometry (ΔGEOM), Core−Valence (CV), full triples (fT), Perturbative Quadruples (pQ), Diagonal Born−Oppenheimer (DBOC), Relativistic (rel), and Spin−Orbit (ΔSO) Contributions to the Energy Barriers *i*ncluded in the HTBH38/08 Database[a]

	reactions	ΔGEOM	CV[b]	fT	pQ	DBOC	rel	ΔSO
HT1	$H^\bullet + HCl \rightarrow H2 + Cl^\bullet$	0.0/1.6	0.1/−0.3 (0.1/−0.3)	−0.3/0.2	−0.1/−0.2	1.6/1.0	−0.5/0.8	0.1/3.5
HT2	$OH^\bullet + H_2 \rightarrow H_2O + H^\bullet$	0.0/0.0	0.0/0.8 (0.0/0.8)	−0.5/−1.1	−0.3/0.3	0.2/1.1	0.0/−0.6	0.8/0.0
HT3	$CH_3^\bullet + H_2 \rightarrow CH_4 + H^\bullet$	0.0/0.0	0.0/0.6 (−0.1/0.6)	−0.2/−0.4	−0.1/−0.1	1.2/1.9	0.0/−0.1	–
HT4	$OH^\bullet + CH_4 \rightarrow CH_3^\bullet + H_2O$	0.0/0.0	0.3/0.4 (0.3/0.4)	−0.1/−0.5	−0.7/−0.1	0.4/0.7	0.0/−0.5	0.8/0.0
HT5	$H^\bullet + H_2 \rightarrow H_2 + H^\bullet$	−0.1/−0.1	0.0/0.0 (0.0/0.0)	−0.3/−0.3	−0.8/−0.8	1.7/1.7	0.0/0.0	–
HT6	$OH^\bullet + NH_3 \rightarrow H_2O + NH_2^\bullet$	−0.2/0.7	0.3/-0.1 (0.4/0.0)	−0.9/−1.0	−1.2/−0.8	1.7/1.5	0.0/−0.2	0.8/0.0
HT7	$HCl + CH_3^\bullet \rightarrow Cl^\bullet + CH_4$	0.0/1.7	0.0/0.3 (0.1/0.3)	0.0/0.4	−0.3/−0.3	0.2/0.3	0.0/1.2	0.0/3.5
HT8	$OH^\bullet + C_2H_6 \rightarrow H_2O + C_2H_5^\bullet$	0.0/0.0	0.2/0.6 (0.2/0.6)	−0.2/−0.4	−0.6/−0.1	−0.3/0.3	−0.2/−0.7	0.8/0.0
HT9	$F^\bullet + H_2 \rightarrow HF + H^\bullet$	0.0/0.0	0.1/0.7 (0.1/0.7)	−0.5/−0.9	−0.2/0.6	0.1/0.9	0.0/−0.8	–
HT10	$^3O + CH_4 \rightarrow OH^\bullet + CH_3^\bullet$	−0.4/−1.3	0.4/0.3 (0.4/0.3)	−0.2/−0.1	−0.2/0.2	0.1/−0.1	0.1/−0.3	0.9/0.8
HT11	$H^\bullet + PH_3 \rightarrow PH_2^\bullet + H_2$	0.0/0.0	−0.1/−0.3 (0.0/−0.4)	−0.5/−0.4	−0.1/−0.2	0.9/0.2	−0.2/0.5	–
HT12	$H^\bullet + OH^\bullet \rightarrow H_2 + {}^3O$	−0.6/0.3	0.4/0.0 (0.4/-0.1)	−0.6/−0.6	0.1/−0.4	1.5/0.9	−0.4/0.1	0.8/0.9
HT13	$H^\bullet + H_2S \rightarrow H_2 + HS^\bullet$	0.0/0.0	0.0/−0.4 (0.0/−0.5)	−0.4/−0.1	−0.1/−0.3	0.9/0.3	−0.3/0.7	0.0/2.3
HT14	$^3O + HCl \rightarrow OH^\bullet + Cl^\bullet$	−0.7/0.1	0.1/0.2 (0.4/0.4)	−2.4/−1.8	−1.3/−0.9	1.4/1.3	−0.4/0.4	0.9/4.3
HT15	$NH_2^\bullet + CH_3^\bullet \rightarrow CH_4 + NH$	−2.5/−1.2	0.4/0.3 (0.4/0.3)	0.0/0.0	−0.3/−0.6	2.0/2.1	−0.2/0.1	–
HT16	$NH_2^\bullet + C_2H_5^\bullet \rightarrow NH + C_2H_6$	−2.6/−1.3	0.5/0.1 (0.5/0.1)	0.3/0.1	−0.4/−0.7	1.1/0.8	−0.2/0.1	–
HT17	$NH_2^\bullet + C_2H_6 \rightarrow NH_3 + C_2H_5^\bullet$	0.0/0.0	0.1/0.9 (0.1/0.9)	0.5/0.3	−0.6/−0.5	0.7/1.5	0.0/−0.3	–
HT18	$NH_2^\bullet + CH_4 \rightarrow NH_3 + CH_3^\bullet$	0.0/0.0	0.1/0.7 (0.1/0.7)	0.5/0.2	−0.6/−0.4	0.8/1.2	0.1/−0.3	–
HT19	s-trans cis−$C_5H_8 \rightarrow$ same	0.01/0.1	0.6/0.6 (0.6/0.6)	0.4/0.4	−1.7/−1.7	0.3/0.3	0.0/0.0	–

[a]All the values are in kJ mol^{-1}. [b]F12a (F12b).

https://doi.org/10.1021/acs.jctc.3c00343
J. Chem. Theory Comput. 2023, 19, 3526−3537

Table 3. Geometry (ΔGEOM), Core−Valence (CV), Full Triples (fT), Perturbative Quadruples (pQ), Diagonal Born−Oppenheimer (DBOC), Relativistic (rel), and Spin−Orbit (ΔSO) Contributions to the Energy Barriers Included in the NHTBH38/08 Database[a]

	reactions	ΔGEOM[b]	CV−F12[c]	fT	pQ	DBOC	rel	ΔSO
NHT1	$H^{\bullet} + N_2O \rightarrow OH^{\bullet} + N_2$	0.2/−0.9	0.6/0.1 (0.6/0.1)	−0.6/1.9	−0.8/−5.1	1.1/0.4	−0.3/0.4	0.0/0.8
NHT2	$H^{\bullet} + FH \rightarrow HF + H^{\bullet}$	0.1/0.1	0.5/0.5 (0.5/0.5)	−0.1/−0.1	−0.4/−0.4	2.3/2.8	−0.7/−0.7	–
NHT3	$H^{\bullet} + ClH \rightarrow HCl + H^{\bullet}$	−0.1/−0.1	0.2/0.2 (0.2/0.2)	−0.4/−0.4	−0.2/−0.2	1.5/1.5	−0.8/−0.8	–
NHT4	$H^{\bullet} + FCH_3 \rightarrow HF + CH_3^{\bullet}$	−0.1/0.0	0.6/1.3 (0.5/1.3)	−0.7/−0.3	−0.7/−0.9	0.7/0.2	−0.7/−0.7	–
NHT5	$H^{\bullet} + F_2 \rightarrow HF + F^{\bullet}$	0.8/0.8	0.1/1.6 (0.1/1.6)	−0.2/0.3	0.3/−2.8	0.7/0.3	−0.1/−1.0	–
NHT6	$CH_3^{\bullet} + FCl \rightarrow CH_3F + Cl^{\bullet}$	0.0/0.0	0.3/1.1 (0.3/1.0)	−0.1/0.0	−0.9/−1.7	0.5/0.6	−0.3/−0.7	0.0/3.5
NHT7	$F^- + CH_3F \rightarrow FCH_3 + F^-$	/	1.5/1.5 (1.5/1.5)	−0.5/−0.5	−0.6/−0.6	0.0/0.0	−0.2/−0.2	–
NHT8	$F^-\cdots CH_3F \rightarrow FCH_3\cdots F^-$	/	1.1/1.1 (1.1/1.1)	−0.3/−0.3	−0.5/−0.5	0.1/0.1	−0.2/−0.2	–
NHT9	$Cl^- + CH_3Cl \rightarrow ClCH_3 + Cl^-$	/	1.2/1.2 (1.4/1.4)	−0.6/−0.6	−0.5/−0.5	0.0/0.0	−0.2/−0.2	–
NHT10	$Cl^-\cdots CH_3Cl \rightarrow ClCH_3\cdots Cl^-$	/	1.1/1.1 (1.2/1.2)	−0.5/−0.5	−0.5/−0.5	0.0/0.0	−0.5/−0.5	–
NHT11	$F^- + CH_3Cl \rightarrow FCH_3 + Cl^-$	/	1.4/0.8 (1.5/0.9)	−0.6/−0.5	−0.4/−0.9	0.0/0.0	−0.2/−0.1	–
NHT12	$F^-\cdots CH_3Cl \rightarrow FCH_3\cdots Cl^-$	/	1.0/0.6 (1.0/0.7)	−0.4/−0.4	0.3/−0.4	0.0/0.0	−0.2/−0.3	–
NHT13	$OH^- + CH_3F \rightarrow HOCH_3 + F^-$	/	1.3/2.0 (1.3/2.0)	−0.3/−0.5	−1.0/−0.9	0.0/0.1	−0.1/−0.5	–
NHT14	$OH^-\cdots CH_3F \rightarrow HOCH_3\cdots F^-$	/	1.1/1.8 (1.1/1.8)	−0.2/−0.6	−0.9/−0.6	0.1/0.1	−0.2/−0.4	–
NHT15	$H^{\bullet} + N_2 \rightarrow HN_2^{\bullet}$	0.0/0.0	0.3/0.4 (0.2/0.4)	−0.5/0.7	1.0/−0.1	1.3/0.4	0.1/−0.4	–
NHT16	$H^{\bullet} + CO \rightarrow HCO^{\bullet}$	0.0/0.0	0.1/1.0 (0.1/1.0)	−0.4/−0.1	−0.2/−0.1	0.8/−0.1	0.0/−0.4	–
NHT17	$H^{\bullet} + C_2H_4 \rightarrow C_2H_5^{\bullet}$	0.0/0.2	0.2/0.0 (0.2/0.0)	−0.5/0.2	0.0/−0.8	0.7/0.0	0.0/−0.2	–
NHT18	$CH_3^{\bullet} + C_2H_4 \rightarrow CH_3CH_2CH_2^{\bullet}$	−0.1/−0.1	0.6/0.6 (0.6/0.6)	−0.8/−1.0	−0.5/−0.8	0.0/0.0	0.0/−0.2	–
NHT19	HCN → HNC	0.1/0.1	1.6/0.8 (1.7/0.8)	−0.6/0.2	0.4/−0.8	0.1/0.2	−0.3/−0.4	–

[a]All the values are in kJ mol^{-1}. [b]the geometries have not been reoptimized at the junChS-F12 level when charged species were involved. [c]F12a (F12b).

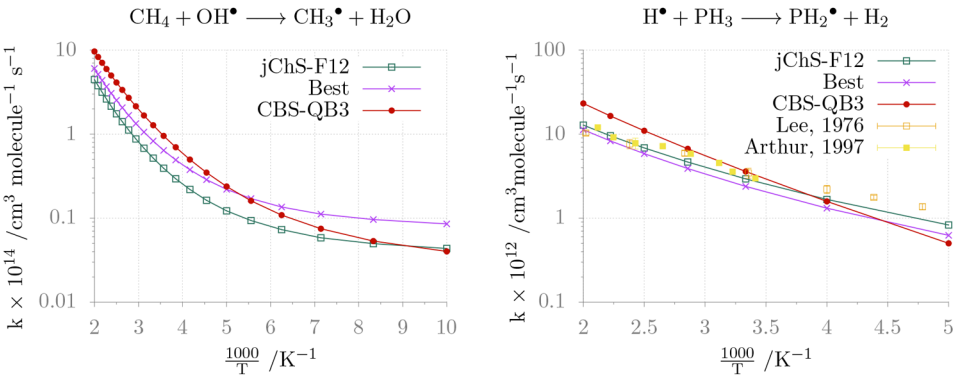

(a) reaction HT4 (b) reaction HT11

Figure 2. Temperature dependence of the rate constants for reactions HT4 and HT11 in the high-pressure limit.

slightly lower value (26.0 kJ mol^{-1} at the W1 level[82]) was estimated in the most exhaustive computation of the rate constant performed until now.[86] In any case, the reaction shows a strongly non-Arrhenius behavior (related also to the presence of a hindered rotation at the transition state) and the agreement between different model chemistries is only fair at low temperatures (see panel (a) of Figure 2). While a more comprehensive analysis of all the factors (path curvature, anharmonicity, etc.) playing a role in determining the rate constant of this reaction is beyond the scope of the present paper, we point out that the difference between harmonic and anharmonic ZPEs is not negligible (about 1 kJ mol^{-1} for both the forward and backward reaction).

Inspection of panel (b) in Figure 2 shows that reaction between H and PH_3 (HT11) follows the Arrhenius behavior. The rate constants computed from junChS-F12 and *Best* energy barriers are in remarkable agreement with the available experimental data,[87,88] whereas the CBS-QB3 energy barrier leads to underestimated rate constants at low temperatures and overestimated rate constants at high temperatures. In this case the role af anharmonicity on the rate constants is negligible: for instance, the difference between harmonic and anharmonic (VPT2) ZPEs is about 0.3 kJ mol^{-1}. All these trends are confirmed by the coefficients of the Arrhenius−Kooij fittings collected in Table 4.

The high pressure limits for the rate constants of reactions NHT10 and NHT19 are shown in Figure 3, while the corresponding Arrhenius-Kooij parameters are given in Table 4. Both reactions are characterized by quite high energy barriers, and their rate constants follow the Arrhenius equation in the medium- to high-temperature range.

Reaction NHT10 is the prototypical S_N2 reaction, which shows very large environmental effects,[89] so that accurate computations of gas phase rate constants are the mandatory prerequisite for disentangling intrinsic and environmental effects. The value of the *Best* energy barrier (9.0 kJ mol^{-1}) coincides with that obtained from the very accurate focal point approach (FPA) given in ref 90. Since tunneling is expected to

https://doi.org/10.1021/acs.jctc.3c00343
J. Chem. Theory Comput. 2023, 19, 3526−3537

Table 4. Arrhenius–Kooij Parameters of the Reactions Investigated in the Present Paper

		junChS-F12	*Best*	CBS-QB3
$CH_4 + OH \rightarrow CH_3 + H_2O$	A/cm^3 molecule^{-1} s^{-1}	3.76×10^{-14}	3.77×10^{-14}	8.19×10^{-14}
	n	2.86	2.86	2.56
	E_a/kJ mol^{-1}	5.31	4.07	4.74
$H + PH_3 \rightarrow PH_2 + H_2$	A/cm^3 molecule^{-1} s^{-1}	9.06×10^{-12}	8.96×10^{-12}	4.84×10^{-11}
	n	2.02	2.03	1.60
	E_a/kJ mol^{-1}	2.85	3.34	6.47
$H + HF \rightarrow HF + H$	A/cm^3 molecule^{-1} s^{-1}	1.75×10^{-16}	1.75×10^{-16}	5.04×10^{-16}
	n	1.81	1.81	1.74
	E_a/kJ mol^{-1}	1.57×10^{2}	1.57×10^{2}	1.63×10^{2}
$Cl^-\cdots CH_3Cl \rightarrow ClCH_3\cdots Cl^-$	A/s^{-1}	1.19×10^{11}	1.19×10^{11}	2.34×10^{11}
	n	1.05	1.06	7.56×10^{-1}
	E_a/kJ mol^{-1}	5.10×10^{1}	5.00×10^{1}	5.07×10^{1}
$HCN \rightarrow HNC$	A/s^{-1}	1.13×10^{14}	8.61×10^{13}	1.78×10^{13}
	n	6.42×10^{-2}	1.93×10^{-1}	1.01
	E_a/kJ mol^{-1}	1.88×10^{2}	1.87×10^{2}	1.82×10^{2}
$C_2H_4 + CN$	A/cm^3 molecule^{-1} s^{-1}	5.89×10^{-10}	5.86×10^{-10}	5.90×10^{-10}
	n	8.55×10^{-2}	5.05×10^{-2}	1.05×10^{-1}
	E_a/kJ mol^{-1}	5.45×10^{-2}	7.73×10^{-2}	4.18×10^{-2}
$CH_2OO + H_2O$	A/cm^3 molecule^{-1} s^{-1}	2.83×10^{-15}	–	2.36×10^{-15}
	n	1.05	–	1.12
	E_a/kJ mol^{-1}	5.63	–	7.30

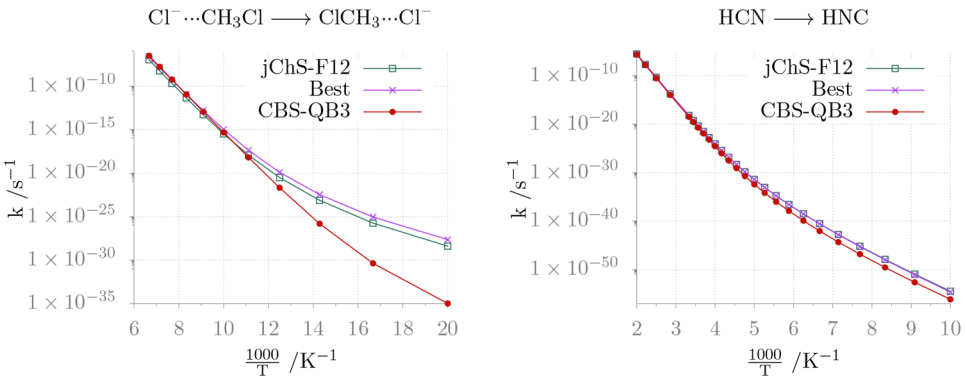

(a) reaction NHT10 (b) reaction NHT19

Figure 3. Temperature dependence of the rate constants for reactions NHT10 and NHT19 in the high-pressure limit.

play a negligible role, accurate rate constants should be obtained at this level. It is then remarkable that *Best* and junChS-F12 rate constants are very close in the whole range of temperatures, whereas the CBS-QB3 model underestimates significantly the rate constant at low temperatures. In fact, the not too high activation energy leads to a significant deviation from the Arrhenius behavior at low temperatures, with the consequent non-negligible impact of even relatively small errors.

The isomerization of HCN to HNC (NHT19) is of paramount relevance in astrochemistry because the ratio between the two species changes in different environments. While the energy barrier is too high to allow effective isomerization in the interstellar medium (ISM), the rate constant of the reaction represents the reference value for studying catalytic effects by water molecules on icy grains.[91] In this case, the rate constants computed by different models are in good agreement in the whole temperature range among themselves and with previous computations.[92]

The last reaction considered (NHT2) is the simplest heavy atom transfer. Figure 4 shows that also in this case, the rate

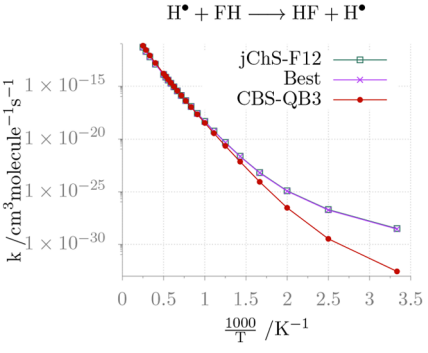

Figure 4. Temperature dependence of the rate constants for reaction NHT2.

constants provided by the different methods are in good agreement for medium- to high-temperatures, whereas at low temperatures the CBS-QB3 energy barriers lead to too low rates in comparison with the (close) values of junChS-F12 and *Best* models.

https://doi.org/10.1021/acs.jctc.3c00343
J. Chem. Theory Comput. 2023, 19, 3526–3537

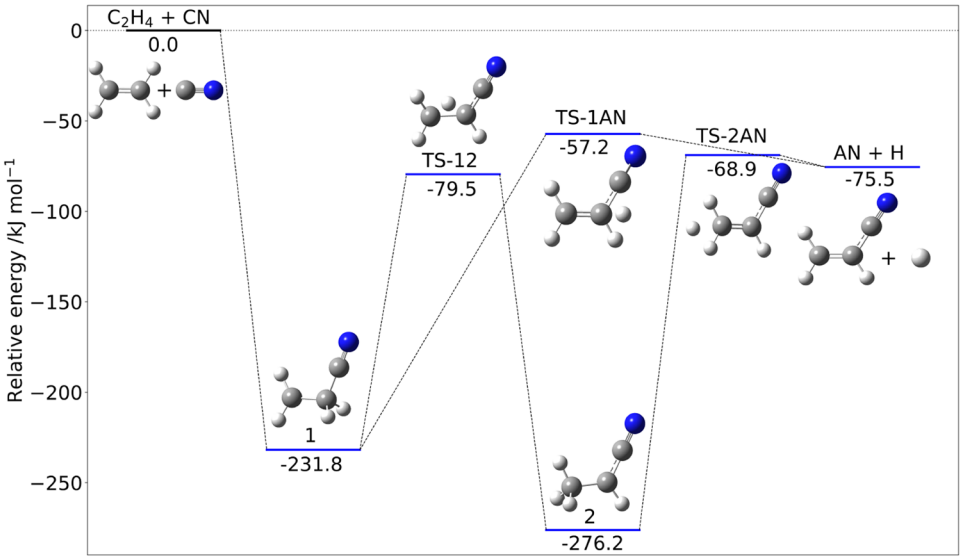

Figure 5. Reaction mechanism for the addition of CN to C_2H_4. Electronic energies at the junChS-F12 level augmented by rDSD anharmonic ZPEs.

In order to investigate the effect of entrance and exit van der Waals wells, two multistep reactions of astrochemical (CN addition to ethylene) and atmospheric (reaction between the simplest Criegee intermediate and H_2O) interest have been investigated.

Aminoacetonitrile (AN), also known as vinylcyanide, has been found in several regions of the ISM[93] and may be also the best candidate for the formation of cell-like membranes in Titan's hydrocarbon-rich lakes and seas.[94] Among the possible formation routes of AN, we have considered the addition of CN radical to ethylene, since both species are present in the ISM and on Titan. From an experimental point of view, the reaction was found to be very fast, approaching the gas kinetics limit at very low and very high temperatures.[95] On the other hand, the computational studies performed until now did not employ state-of-the-art quantum chemical models.[96] The reaction mechanism is sketched in Figure 5 together with the junChS-F12 relative energies (including rDSD anharmonic ZPEs) of all the stationary points.

Intermediate 1, which is formed without any entrance barrier, leads to the final products (H and AN), either through a single step ruled by the transition state TS-1AN or by a two-step mechanism involving intermediate 2. In any case, all the energy barriers are submerged, so that this reaction channel is open also in the harsh conditions characterizing the ISM.

The rate constant for the addition issued from junChS-F12 computations is compared in Figure 6 with the CBS-QB3 and *Best* counterparts. The addition rate constant is essentially flat in the whole temperature range and the different composite methods provide comparable results. Although a fully quantitative comparison with experimental rate constants is not possible because we have considered only the high pressure limit, our values have the correct order of magnitude, especially at high temperatures.[95]

Criegee intermediates (CIs) are carbonyl oxides formed in the ozonolysis of unsaturated hydrocarbons and play a central role in several processes occurring in the atmosphere. Reaction with water is a key step for several processes involving CIs and has been investigated in a number of studies. In particular, the rate constant for the reaction of the simplest CI (CH_2OO) has been analyzed in a thorough computational study.[97]

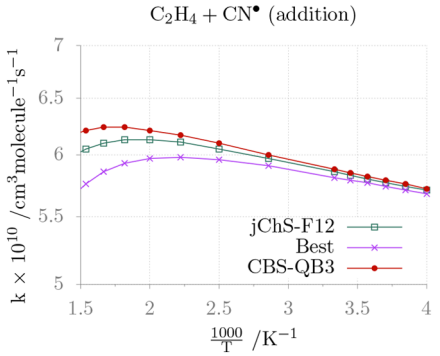

Figure 6. Temperature dependence of the rate constant for the addition of CN to C_2H_4 in the high pressure limit.

The reaction mechanism is sketched in Figure 7 together with the relative energies of the key stationary points

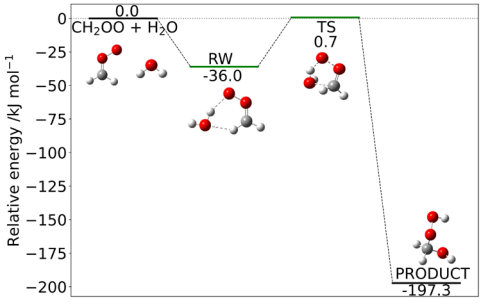

Figure 7. Mechanism of the reaction between CH_2OO and H_2O. Electronic energies at the junChS-F12 level augmented by anharmonic rDSD ZPEs.

computed at the junChS-F12 level and including anharmonic ZPEs computed at the rDSD level. The rate constants predicted by different composite methods in the framework of the ME/TST model are shown in Figure 8. In this case the temperature dependence of the rate constant is well represented by the simple Arrhenius equation, but the slope is significantly different when employing junChS-F12 or CBS-

https://doi.org/10.1021/acs.jctc.3c00343
J. Chem. Theory Comput. 2023, 19, 3526−3537

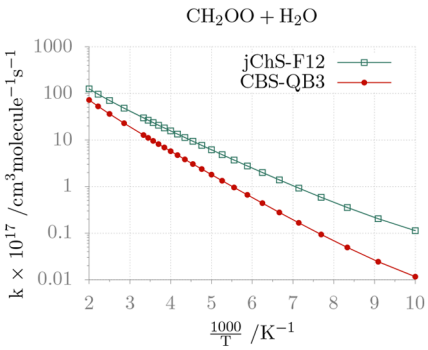

Figure 8. Temperature dependence of the rate constant of the reaction between CH_2OO and H_2O in the high pressure limit.

QB3 energy barriers. Once again all these trends are confirmed quantitatively by the coefficients of the Arrhenius–Kooij fittings given in Table 4 and the junChS-F12 results are in agreement with previous state-of-the-art computations.[97]

CONCLUSIONS

The analysis of processes occurring in nonstandard environments like the atmospheres of exoplanets or the Earth's troposphere requires accurate kinetic data at low to moderate temperatures and involving barrier heights spanning a large range of values. Furthermore, medium- to large-molecular systems are often involved in those processes, whose entrance channels are tuned by noncovalent interactions. As a consequence, reliable yet effective methods for the computation of rate constants and branching ratios are needed. The master equation formalism employing the ab initio transition state theory offers a reliable reference frame, provided that accurate structural and energetic parameters are available for the key stationary points. To this end, we have validated the recently proposed junChS-F12 model chemistry with reference to very accurate energetic and kinetic data. The results obtained for a large panel of systems and reaction channels show an average error well within the chemical accuracy for all the key thermodynamic and kinetic contributions without the need of any empirical parameter. The junChS-F12 model delivers smaller errors with respect to the reference values than its conventional junChS predecessor, without any excessive increase of computational resources. This behavior can be traced back to the strongly reduced role of CBS extrapolation when going from conventional to explicitly correlated composite methods, with the consequent reduced role of the errors incurred from its estimation by low-order perturbative methods. The computational bottleneck of the proposed model chemistry is the CCSD(T)-F12/jun-cc-pVTZ step. In this connection, new low-scaling approaches[98] and, possibly, local-correlation models[99,100] deserve further investigation in order to increase the dimension of molecular systems amenable to accurate computations with reasonable computer requirements. Additional refinements and validations are needed also for situations involving the non-negligible static correlation and/or nonadiabatic effects. However, even taking these limitations into account, we think that the strategy proposed in the present paper can contribute to the computational study of chemical processes under widely different temperature and pressure conditions.

ASSOCIATED CONTENT

Supporting Information

The Supporting Information is available free of charge at https://pubs.acs.org/doi/10.1021/acs.jctc.3c00343.

Additional data for energy barriers (PDF)

AUTHOR INFORMATION

Corresponding Author

Vincenzo Barone − *SMART Laboratory, Scuola Normale Superiore di Pisa, 56125 Pisa, Italy;* orcid.org/0000-0001-6420-4107; Email: vincenzo.barone@sns.it

Authors

Jacopo Lupi − *SMART Laboratory, Scuola Normale Superiore di Pisa, 56125 Pisa, Italy;* orcid.org/0000-0001-6522-9947

Zoi Salta − *SMART Laboratory, Scuola Normale Superiore di Pisa, 56125 Pisa, Italy;* orcid.org/0000-0002-7826-0182

Nicola Tasinato − *SMART Laboratory, Scuola Normale Superiore di Pisa, 56125 Pisa, Italy;* orcid.org/0000-0003-1755-7238

Complete contact information is available at: https://pubs.acs.org/10.1021/acs.jctc.3c00343

Notes

The authors declare no competing financial interest.

ACKNOWLEDGMENTS

Funding from the Italian Ministry of University and Research (MUR, Grant 2017A4XRCA) and Italian Space Agency (ASI, "Life in Space" project no. 2019-3-U.0) is gratefully acknowledged.

REFERENCES

(1) Coker, A. K. *Modeling of chemical kinetics and reactor design*; Gulf Professional Publishing, 2001.

(2) Lin, K. H. Applied Kinetics - Part I. *Ind. Eng. Chem.* **1968**, *60*, 61–82.

(3) Vereecken, L.; Francisco, J. S. Theoretical studies of atmospheric reaction mechanisms in the troposphere. *Chem. Soc. Rev.* **2012**, *41*, 6259–6293.

(4) Arrhenius, S. On the Reaction Velocity of the Inversion of Cane Sugar by Acids. *Z. Phys. Chem.* **1889**, *4*. DOI: 10.1515/zpch-1889-0116

(5) Tolman, R. C. *Statistical Mechanics with Applications to Physics and Chemistry*; The Chemical Catalog Company, Inc., 1927.

(6) Truhlar, D. G. Interpretation of the activation energy. *J. Chem. Educ.* **1978**, *55*, 309.

(7) Levitt, B. P.; Smith, I. W. *Physical chemistry of fast reactions*; Springer, 1973; Vol. *1*.

(8) Smith, I. W. *Kinetics and Dynamics of Elementary Gas Reactions*; Butterworth-Heinemann, 1980.

(9) Császár, A. G.; Allen, W. D.; Schaefer, H. F. In pursuit of the ab initio limit for conformational energy prototypes. *J. Chem. Phys.* **1998**, *108*, 9751–9764.

(10) Curtiss, L. A.; Redfern, P. C.; Raghavachari, K. Assessment of Gaussian-4 theory for energy barriers. *Chem. Phys. Lett.* **2010**, *499*, 168–172.

(11) Guner, V.; Khuong, K. S.; Leach, A. G.; Lee, P. S.; Bartberger, M. D.; Houk, K. N. A Standard Set of Pericyclic Reactions of Hydrocarbons for the Benchmarking of Computational Methods: The Performance of ab Initio, Density Functional, CASSCF, CASPT2, and CBS-QB3Methods for the Prediction of Activation Barriers, Reaction Energetics, and Transition State Geometries. *J. Phys. Chem. A* **2003**, *107*, 11445–11459.

(12) Karton, A.; Martin, J. M. L. Explicitly correlated Wn theory: W1-F12 and W2-F12. *J. Chem. Phys.* **2012**, *136*, 124114.
(13) Ventura, O. N.; Kieninger, M.; Katz, A.; Vega-Teijido, M.; Segovia, M.; Irving, K. SVECV-F12: benchmark of a composite scheme for accurate and cost effective evaluation of reaction barriers. *Int. J. Quantum Chem.* **2021**, *121*, e26745.
(14) Tajti, A.; Szalay, P. G.; Császár, A. G.; Kállay, M.; Gauss, J.; Valeev, E. F.; Flowers, B. A.; Vázquez, J.; Stanton, J. F. HEAT: High accuracy extrapolated ab initio thermochemistry. *J. Chem. Phys.* **2004**, *121*, 11599−11613.
(15) Sylvetsky, N.; Peterson, K. A.; Karton, A.; Martin, J. M. Toward a W4-F12 approach: Can explicitly correlated and orbital-based ab initio CCSD(T) limits be reconciled? *J. Chem. Phys.* **2016**, *144*, 214101.
(16) Barone, V.; Lupi, J.; Salta, Z.; Tasinato, N. Development and Validation of a Parameter-Free Model Chemistry for the Computation of Reliable Reaction Rates. *J. Chem. Theory Comput.* **2021**, *17*, 4913−4928.
(17) Puzzarini, C.; Barone, V. Extending the molecular size in accurate quantum-chemical calculations: the equilibrium structure and spectroscopic properties of uracil. *Phys. Chem. Chem. Phys.* **2011**, *13*, 7189−7197.
(18) Puzzarini, C.; Biczysko, M.; Barone, V.; Peña, I.; Cabezas, C.; Alonso, J. L. Accurate molecular structure and spectroscopic properties of nucleobases: a combined computational-microwave investigation of 2-thiouracil as a case study. *Phys. Chem. Chem. Phys.* **2013**, *15*, 16965−16975.
(19) Puzzarini, C.; Biczysko, M.; Barone, V.; Largo, L.; Peña, I.; Cabezas, C.; Alonso, J. L. Accurate Characterization of the Peptide Linkage in the Gas Phase: a Joint Quantum-chemical and Rotational Spectroscopy Study of the Glycine Dipeptide Analogue. *J. Phys. Chem. Lett.* **2014**, *5*, 534−540.
(20) Salta, Z.; Tasinato, N.; Lupi, J.; Boussessi, R.; Balbi, A.; Puzzarini, C.; Barone, V. Exploring the Maze of $C_2N_2H_5$ Radicals and Their Fragments in the Interstellar Medium with the Help of Quantum-Chemical Computations. *ACS Earth Space Chem.* **2020**, *4*, 774−782.
(21) Lupi, J.; Puzzarini, C.; Cavallotti, C.; Barone, V. State-of-the-Art Quantum Chemistry Meets Variable Reaction Coordinate Transition State Theory to Solve the Puzzling Case of the H_2S + Cl System. *J. Chem. Theory Comput.* **2020**, *16*, 5090−5104.
(22) Lupi, J.; Puzzarini, C.; Barone, V. Methanimine as a Key Precursor of Imines in the Interstellar Medium: The Case of Propargylimine. *Astrophys. J. Lett.* **2020**, *903*, L35.
(23) Ballotta, B.; Nandi, S.; Barone, V.; Rampino, S. Gas-Phase Formation and Isomerization Reactions of Cyanoacetaldehyde, a Prebiotic Molecule of Astrochemical Interest. *ACS Earth Space Chem.* **2021**, *5*, 1071−1082.
(24) Baiano, C.; Lupi, J.; Tasinato, N.; Puzzarini, C.; Barone, V. The Role of State-of-the-Art Quantum-Chemical Calculations in Astrochemistry: Formation Route and Spectroscopy of Ethanimine as a Paradigmatic Case. *Molecules* **2020**, *25*, 2873.
(25) Chan, B.; Radom, L. W1X-1 and W1X-2: W1-Quality Accuracy with an Order of Magnitude Reduction in Computational Cost. *J. Chem. Theory Comput.h* **2012**, *8*, 4259−4269.
(26) Møller, C.; Plesset, M. S. Note on an Approximation Treatment for Many-Electron Systems. *Phys. Rev.* **1934**, *46*, 618−622.
(27) DeYonker, N. J.; Cundari, T. R.; Wilson, A. K. The Correlation Consistent Composite Approach (ccCA): an Alternative to the Gaussian-n Methods. *J. Chem. Phys.* **2006**, *124*, 114104.
(28) DeYonker, N. J.; Wilson, B. R.; Pierpont, A. W.; Cundari, T. R.; Wilson, A. K. Towards the Intrinsic Error of the Correlation Consistent Composite Approach (ccCA). *Mol. Phys.* **2009**, *107*, 1107−1121.
(29) Papajak, E.; Zheng, J.; Xu, X.; Leverentz, R. H.; Truhlar, G. D. Perspectives on Basis Sets Beautiful: Seasonal Plantings of Diffuse Basis Functions. *J. Chem. Theory Comput.* **2011**, *7*, 3027−3034.
(30) Alessandrini, S.; Barone, V.; Puzzarini, C. Extension of the "Cheap" Composite Approach to Noncovalent Interactions: The jun-ChS Scheme. *J. Chem. Theory Comput.* **2020**, *16*, 988−1006.
(31) Melli, A.; Barone, V.; Puzzarini, C. Unveiling Bifunctional Hydrogen Bonding with the Help of Quantum Chemistry: The Imidazole-Water Adduct as Test Case. *J. Phys. Chem. A* **2021**, *125*, 2989−2998.
(32) Lupi, J.; Alessandrini, S.; Barone, V.; Puzzarini, C. junChS and junChS-F12 Models: Parameter-free Efficient yet Accurate Composite Schemes for Energies and Structures of Noncovalent Complexes. *J. Chem. Theory Comput.* **2021**, *17*, 6974−6992.
(33) Barone, V.; Fusè, M.; Lazzari, F.; Mancini, G. Benchmark Structures and Conformational Landscapes of Amino Acids in the Gas Phase: a Joint Venture of Machine Learning, Quantum Chemistry, and Rotational Spectroscopy. *J. Chem. Theory Comput.* **2023**, *19*, 1243−1260.
(34) Bao, J. L.; Truhlar, D. G. Variational transition state theory: theoretical framework and recent developments. *Chem. Soc. Rev.* **2017**, *46*, 7548−7596.
(35) Miller, A. J.; Klippenstein, J. S. Master equation methods in gas phase chemical kinetics. *J. Phys. Chem. A* **2006**, *110*, 10528−10544.
(36) Klippenstein, S. J. From Theoretical Reaction Dynamics to Chemical Modeling of Combustion. *Proc. Combust. Inst.* **2017**, *36*, 77−111.
(37) Dunning, T. H., Jr. Gaussian basis sets for use in correlated molecular calculations. I. The atoms boron through neon and hydrogen. *J. Chem. Phys.* **1989**, *90*, 1007−1023.
(38) Santra, G.; Sylvetsky, N.; Martin, J. M. Minimally empirical double-hybrid functionals trained against the GMTKN55 database: revDSD-PBEP86-D4, revDOD-PBE-D4, and DOD-SCAN-D4. *J. Phys. Chem. A* **2019**, *123*, 5129−5143.
(39) Biczysko, M.; Panek, P.; Scalmani, G.; Bloino, J.; Barone, V. Harmonic and Anharmonic Vibrational Frequency Calculations with the Double-Hybrid B2PLYP Method: Analytic Second Derivatives and Benchmark Studies. *J. Chem. Theory Comput.* **2010**, *6*, 2115−2125.
(40) Knizia, G.; Adler, T. B.; Werner, H.-J. Simplified CCSD(T)-F12 methods: Theory and benchmarks. *J. Chem. Phys.* **2009**, *130*, 054104.
(41) Adler, T. B.; Knizia, G.; Werner, H.-J. A simple and efficient CCSD (T)-F12 approximation. *J. Chem. Phys.* **2007**, *127*, 221106.
(42) Moore, C. E. *Atomic Energy Levels*; Natl. Bur. Stand. (US) Circ, 1949.
(43) Frisch, M. J.; et al. *Gaussian Inc 16 Revision C.01*; Gaussian Inc.: Wallingford, CT, 2016.
(44) Werner, H.-J.; et al. The Molpro quantum chemistry package. *J. Chem. Phys.* **2020**, *152*, 144107.
(45) Kállay, M.; et al. *MRCC, a quantum chemical program suite*; MRCC, 2018.
(46) Stanton, J. F.; Gauss, J.; Harding, M. E.; Szalay, P. G. *CFOUR. A quantum chemical program package*. 2016; with contributions from A. A. Auer, R. J. Bartlett, U. Benedikt, C. Berger, D. E. Bernholdt, Y. J. Bomble, O. Christiansen, F. Engel, M. Heckert, O. Heun, C. Huber, T.-C. Jagau, D. Jonsson, J. Jusélius, K. Klein, W. J. Lauderdale, F. Lipparini, D. Matthews, T. Metzroth, L. A. Mück, D. P. O'Neill, D. R. Price, E. Prochnow, C. Puzzarini, K. Ruud, F. Schiffmann, W. Schwalbach, S. Stopkowicz, A. Tajti, J. Vázquez, F. Wang, J. D. Watts and the integral packages MOLECULE (J. Almlöf and P. R. Taylor), PROPS (P. R. Taylor), ABACUS (T. Helgaker, H. J. Aa. Jensen, P. Jørgensen, and J. Olsen), and ECP routines by A. V. Mitin and C. van Wüllen. For the current version, see http://www.cfour.de.
(47) Helgaker, T.; Klopper, W.; Koch, H.; Noga, J. Basis-set convergence of correlated calculations on water. *J. Chem. Phys.* **1997**, *106*, 9639−9646.
(48) Woon, D. E.; Dunning, T. H., Jr. Gaussian Basis Sets for Use in Correlated Molecular Calculations. V. Core-Valence Basis Sets for Boron through Neon. *J. Chem. Phys.* **1995**, *103*, 4572−4585.

https://doi.org/10.1021/acs.jctc.3c00343
J. Chem. Theory Comput. 2023, 19, 3526−3537

(49) Heckert, M.; Kállay, M.; Gauss, J. Molecular Equilibrium Geometries Based on Coupled-Cluster Calculations Including Quadruple Excitations. *Mol. Phys.* **2005**, *103*, 2109−2115.
(50) Heckert, M.; Kállay, M.; Tew, D. P.; Klopper, W.; Gauss, J. Basis-Set Extrapolation Techniques for the Accurate Calculation of Molecular Equilibrium Geometries Using Coupled-Cluster Theory. *J. Chem. Phys.* **2006**, *125*, 044108.
(51) Barone, V.; Di Grande, S.; Puzzarini, C. Toward accurate yet effective computations of rotational spectroscopy parameters for biomolecule building blocks. *Molecules* **2023**, *28*, 913.
(52) Puzzarini, C.; Bloino, J.; Tasinato, N.; Barone, V. Accuracy and interpretability: The devil and the holy grail. New routes across old boundaries in computational spectroscopy. *Chem. Rev.* **2019**, *119*, 8131−8191.
(53) Barone, V.; Puzzarini, C. Gas-Phase Computational Spectroscopy: The Challenge Of The Molecular Bricks Of Life. *Annu. Rev. Phys. Chem.* **2023**, *74*, 29−52.
(54) Sellers, H.; Pulay, P. The adiabatic correction to molecular potential surfaces in the SCF approximation. *Chem. Phys. Lett.* **1984**, *103*, 463−465.
(55) Handy, N. C.; Yamaguchi, Y.; Schaefer, H. F. The diagonal correction to the Born-Oppenheimer approximation: Its effect on the singlet-triplet splitting of CH_2 and other molecular effects. *J. Chem. Phys.* **1986**, *84*, 4481−4484.
(56) Handy, N. C.; Lee, A. M. The adiabatic approximation. *Chem. Phys. Lett.* **1996**, *252*, 425−430.
(57) Kutzelnigg, W. The adiabatic approximation I. The physical background of the Born-Handy ansatz. *Mol. Phys.* **1997**, *90*, 909−916.
(58) Cowan, R. D.; Griffin, M. Approximate relativistic corrections to atomic radial wave functions. *J. Opt. Soc. Am.* **1976**, *66*, 1010−1014.
(59) Martin, R. L. All-electron relativistic calculations on silver hydride. An investigation of the Cowan-Griffin operator in a molecular species. *J. Phys. Chem.* **1983**, *87*, 750−754.
(60) Irikura, K. K.; Johnson, R.; Kacker, R. N.; Kessel, R. Uncertainties in scaling factors for ab initio vibrational zero-point energies. *J. Chem. Phys.* **2009**, *130*, 114102.
(61) Barone, V. Anharmonic vibrational properties by a fully automated second order perturbative approach. *J. Chem. Phys.* **2005**, *122*, 014108.
(62) Skouteris, D.; Calderini, D.; Barone, V. Methods for calculating partition functions of molecules involving large amplitude and/or anharmonic motions. *J. Chem. Theory Comput.* **2016**, *12*, 1011−1018.
(63) Schuurman, M. S.; Allen, W. D.; von Ragué Schleyer, P.; Schaefer, H. F. I. The highly anharmonic BH_5 potential energy surface characterized in the ab initio limit. *J. Chem. Phys.* **2005**, *122*, 104302.
(64) Piccardo, M.; Bloino, J.; Barone, V. Generalized vibrational perturbation theory for rotovibrational energies of linear, symmetric and asymmetric tops: Theory, approximations, and automated approaches to deal with medium-to-large molecular systems. *Int. J. Quantum Chem.* **2015**, *115*, 948−982.
(65) Bloino, J.; Biczysko, M.; Barone, V. General perturbative approach for spectroscopy, thermodynamics and kinetics: methodological background and benchmark studies. *J. Chem. Theory Comput.* **2012**, *8*, 1015−1036.
(66) Ayala, P. Y.; Schlegel, H. B. Identification and treatment of internal rotation in normal mode vibrational analysis. *J. Chem. Phys.* **1998**, *108*, 2314−2325.
(67) Barone, V.; Biczysko, M.; Bloino, J. Fully anharmonic IR and Raman spectra of medium-size molecular systems: accuracy and interpretation. *Phys. Chem. Chem. Phys.* **2014**, *16*, 1759−1787.
(68) Truhlar, D. G.; Isaacson, A. D. Simple perturbation theory estimates of equilibrium constants from force fields. *J. Chem. Phys.* **1991**, *94*, 357−359.
(69) Tardy, D. C.; Rabinovitch, B. Collisional Energy Transfer. Thermal Unimolecular Systems in the Low-Pressure Region. *J. Chem. Phys.* **1966**, *45*, 3720−3730.
(70) Fernández-Ramos, A.; Miller, J. A.; Klippenstein, S. J.; Truhlar, D. G. Modeling the Kinetics of Bimolecular Reactions. *Chem. Rev.* **2006**, *106*, 4518−4584.
(71) Eckart, C. The penetration of a potential barrier by electrons. *Phys. Rev.* **1930**, *35*, 1303−1309.
(72) Hunter, M.; Reid, S. A.; Robie, D. C.; Reisler, H. The Monoenergetic Unimolecular Reaction of Expansion-Cooled NO_2: NO Product State Distributions at Excess Energies 03000 cm^{-1}. *J. Chem. Phys.* **1993**, *99*, 1093−1108.
(73) Skouteris, D.; Balucani, N.; Ceccarelli, C.; Vazart, F.; Puzzarini, C.; Barone, V.; Codella, C.; Lefloch, B. The Genealogical Tree of Ethanol: Gas-phase Formation of Glycolaldehyde, Acetic Acid, and Formic Acid. *Astrophys. J.* **2018**, *854*, 135.
(74) Gao, L. G.; Zheng, J.; Fernandez-Ramos, A.; Truhlar, D. G.; Xu, X. Kinetics of the Methanol Reaction with OH at Interstellar, Atmospheric and Combustion Temperatures. *J. Am. Chem. Soc.* **2018**, *140*, 2906−2918.
(75) Kooij, D. M. Über die Zersetzung des gasförmigen Phosphorwasserstoffs. *Zeitschr. Phys. Chem.* **1893**, *12U*, 155−161.
(76) Laidler, K. A. A glossary of terms used in chemical kinetics, including reaction dynamics (IUPAC recommendations 1996). *Pure Appl. Chem.* **1996**, *68*, 149−192.
(77) Karton, A.; Tarnopolsky, A.; Lamère, J.; Schatz, G. C.; Martin, J. M. L. Highly Accurate First-Principles Benchmark Data Sets for the Parametrization and Validation of Density Functional and Other Approximate Methods. Derivation of a Robust, Generally Applicable, Double-Hybrid Functional for Thermochemistry and Thermochemical Kinetics. *J. Phys. Chem. A* **2008**, *112*, 12868−12886.
(78) Zheng, J.; Zhao, Y.; Truhlar, D. G. The DBH24/08 Database and Its Use to Assess Electronic Structure Model Chemistries for Chemical Reaction Barrier Heights. *J. Chem. Theory Comput.* **2009**, *5*, 808−821.
(79) Karton, A.; Rabinovich, E.; Martin, J. M. L.; Ruscic, B. W4 Theory for computational thermochemistry: in pursuit of confident sub-kJ/mol predictions. *J. Chem. Phys.* **2006**, *125*, 144108.
(80) Zhao, Y.; Lynch, B. J.; Truhlar, D. G. Multi-coefficient extrapolated density functional theory for thermochemistry and thermochemical kinetics. *Phys. Chem. Chem. Phys.* **2005**, *7*, 43−52.
(81) Zhao, Y.; González-García, N.; Truhlar, D. G. Benchmark Database of Barrier Heights for Heavy Atom Transfer, Nucleophilic Substitution, Association, and Unimolecular Reactions and Its Use to Test Theoretical Methods. *J. Phys. Chem. A* **2005**, *109*, 2012−2018.
(82) Parthiban, S.; Martin, J. M. L. Assessment of W1 and W2 theories for the computation of electron affinities, ionization potentials, heats of formation, and proton affinities. *J. Chem. Phys.* **2001**, *114*, 6014.
(83) Menon, A. S.; Radom, L. Consequences of Spin Contamination in Unrestricted Calculations on Open-Shell Species: Effect of Hartree Fock and Møller Plesset Contributions in Hybrid and Double-Hybrid Density Functional Theory Approaches. *J. Phys. Chem. A* **2008**, *112*, 13225−13230.
(84) Cohen, A. J.; Tozer, D. J.; Handy, N. C. Evaluation of S^2 in density functional theory. *J. Chem. Phys.* **2007**, *126*, 214104.
(85) Hein, R.; Crutzen, P. J.; Heimann, M. An inverse modeling approach to investigate the global atmospheric methane cycle. *Global Biogeochem. Cycles* **1997**, *11*, 43−76.
(86) Ellingson, B. A.; Pu, J.; Lin, H.; Zhao, Y.; Truhlar, D. G. Multicoefficient Gaussian-3 calculation of the rate constant for the OH + CH_4 reaction and its 12C/13C kinetic isotope effect with emphasis on the effects of coordinate system and torsional treatment. *J. Phys. Chem. A* **2007**, *111*, 11706−11717.
(87) Lee, J. H.; Michael, J. V.; Payne, W. A.; Whytock, D. A.; Stief, L. J. Absolute rate constant for the reaction of atomic hydrogen with phosphine over the temperature range 209 to 495 K. *J. Chem. Phys.* **1976**, *65*, 3280−3283.
(88) Arthur, N. L.; Cooper, I. A. Arrhenius parameters for the reactions of H atoms with PH_3 and AsH_3. *J. Chem. Soc., Faraday Trans.* **1997**, *93*, 521−524.

https://doi.org/10.1021/acs.jctc.3c00343
J. Chem. Theory Comput. 2023, 19, 3526−3537

(89) Tirado-Rives, J.; Jorgensen, W. L. QM/MM Calculations for the Cl^- + CH_3Cl S_N2 Reaction in Water Using CM5 Charges and Density Functional Theory. *J. Phys. Chem. A* **2019**, *123*, 5713−5717.
(90) Gonzales, H. M.; Allen, W. D.; Schaefer, H. F., III Model Identity S_N2 Reactions $CH_3X + X^-$ (X = F, Cl, CN, OH, SH, NH_2, PH_2): Marcus Theory Analyzed. *J. Phys. Chem. A* **2005**, *109*, 10613−10628.
(91) Baiano, C.; Lupi, J.; Barone, V.; Tasinato, N. Gliding on ice in search of accurate and cost-effective computational methods for astrochemistry on grains: the puzzling case of the HCN isomerization. *J. Chem. Theory Comput.* **2022**, *18*, 3111−3121.
(92) Isaacson, A. D. Including Anharmonicity in the Calculation of Rate Constants. 1. The HCN/HNC Isomerization Reaction. *J. Phys. Chem. A* **2006**, *110*, 379−388.
(93) Agundez, M.; Fonfria, J. P.; Cernicharo, J.; Pardo, J. R.; Guelin, M. Detection of circumstellar CH_2CHCN, CH_2CN, CH_3CCH, and H_2CS. *Astron. Astrophys.* **2008**, *479*, 493−501.
(94) Sharma, M. K. Vinyl cyanide (CH_2CHCN) in interstellar space: potential spectral lines for its detection. *Heliyon* **2019**, *5*, e02384.
(95) Saidani, G.; Kalugina, Y.; Gardez, A.; Biennier, L.; Georges, R.; Lique, F. High Temperature Reaction Kinetics of CN(ν = 0) with C_2H_4 and C_2H_6 and Vibrational Relaxation of CN(ν = 1) with Ar and He. *J. Chem. Phys.* **2013**, *138*, 124308.
(96) Balucani, N.; Leonori, F.; Petrucci, R.; Wang, X.; Casavecchia, P.; Skouteris, D.; Albernaz, A. F.; Gargano, R. A Combined Crossed Molecular Beams and Theoretical Study of the Reaction CN + C_2H_4. *Chem. Phys.* **2015**, *449*, 34−42.
(97) Long, B.; Bao, J. L.; Truhlar, D. G. Atmospheric chemistry of Criegee intermediates: unimolecular reactions and reactions with water. *J. Am. Chem. Soc.* **2016**, *138*, 14409−14422.
(98) Kallay, M.; Horvath, R. A.; Gyevi-Nagy, L.; Nagy, P. R. Basis Set Limit CCSD(T) Energies for Extended Molecules via a Reduced-Cost Explicitly Correlated Approach. *J. Chem. Theory Comput.* **2023**, *19*, 174−189.
(99) Nagy, P. R.; Kallay, M. Approaching the basis set limit of CCSD(T) energies for large molecules with local natural orbital coupled-cluster methods. *J. Chem. Theory Comput.* **2019**, *15*, 5275−5298.
(100) Liakos, D. G.; Guo, Y.; Neese, F. Comprehensive benchmark results for the domain based local pair natural orbital coupled cluster method (DLPNO-CCSD(T)) for closed- and open-shell systems. *J. Phys. Chem. A* **2020**, *124*, 90−100.

https://doi.org/10.1021/acs.jctc.3c00343
J. Chem. Theory Comput. 2023, 19, 3526−3537